SISSA

PAPER

On the role of intrinsic noise on the response of the p53-Mdm2 module

View the article online for updates and enhancements.

Related content

- Exploring a minimal two-component p53 model
  Tingzhe Sun, Ruoshi Yuan, Wei Xu et al.

- Oscillations and temporal signalling in cells
  G Tiana, S Krishna, S Pigolotti et al.

- The dynamics of p53 in single cells: physiologically based ODE and reaction–diffusion PDE models
  Ján Eliaš, Luna Dimitrio, Jean Clairambault et al.

Recent citations

- A novel mathematical model of ATM/p53/NF- B pathways points to the importance of the DDR switch-off mechanisms
  Katarzyna Jonak *et al*
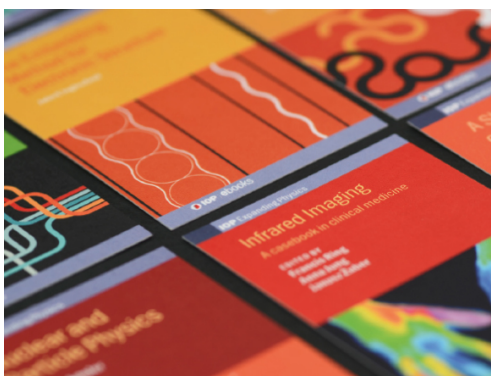
On the role of intrinsic noise on the response of the p53-Mdm2 module

Lídice Cruz-Rodríguez[1], Nuris Figueroa-Morales[2, 3] and Roberto Mulet[4]

[1] Group of Complex Systems and Statistical Physics and Department of General Physics, Physics Faculty, University of Havana, CP 10400, La Habana, Cuba

[2] Group of Complex Systems and Statistical Physics, Physics Faculty, University of Havana, CP 10400, Cuba

[3] PMMH, UMR 7636 ESPCI-Université Pierre et Marie Curie, 10 rue Vauquelin, 75231 Paris Cedex 5, France

[4] Group of Complex Systems and Statistical Physics and Department of Theoretical Physics, Physics Faculty, University of Havana, La Habana, CP 10400, Cuba

E-mail: lcruz@fisica.uh.cu and mulet@fisica.uh.cu

Abstract. The protein p53 has a well established role in protecting genomic integrity in human cells. When DNA is damaged p53 induces the cell cycle arrest to prevent the transmission of the damage to cell progeny, triggers the production of proteins for DNA repair and if the damage can not be repaired the p53-mediated apoptotic pathway is ultimately activated. The p53-Mdm2 feedback loop seems to be the key circuit in this response of cells to damage. Measurements in individual human cells have shown that p53 and its regulator Mdm2 develop sustained oscillations over long periods of time, even in the absence of stress. Here we study three stochastic models of the p53-Mdm2 circuit. The models capture the response of the p53-Mdm2 circuit in its basal state, in the presence of DNA damage, and under oncogenic signals. They are studied through Gillespie's simulations, mean field methods and analytical approaches within the context of the linear noise approximation. While we can not discard that other sources of noise may also be important, our results compare *quantitatively* well with existing experimental data in single cells, supporting the relevance of the intrinsic noise in tuning cellular functions.

Contents

Introduction

The p53 protein has attracted special attention during the last twenty years due to strong existing evidence of its malfunction in most human cancers [1]. Like most proteins, p53 may be inactivated directly by mutations in its own gene or as a result of the interactions with other genes that transmit information to or from p53. Unfortunately, the many pathways that control its activation and the comparable large number of functions, some apparently contradictory, still make the complete understanding of the role played by this protein an unsolved problem [1, 2].

In general, p53 works as a transcription factor that positively or negatively regulates the expression of several, and very different genes. The p53 gene was first identified as a tumor suppressor gene, but we have now evidence that it has a role in the regulation of glycolysis [3], the repair of oncogenic response [4], the regulation of metabolism [5] and many others [2].

One of the main mechanisms regulating the expression of p53 is its interaction with the protein Mdm2. They form together a feedback loop very common in many biological systems. In normal conditions the activation of p53 activates Mdm2 that in turn suppresses p53 [6]. Then, if the cell is in the presence of stress, like DNA damage, p53 and/or Mdm2 are phosphorylated and their interaction is reduced, increasing the level of p53 in the cell [6].

The first experimental studies of the dynamics of p53 and Mdm2 after gamma irradiation were done studying the *average* concentration of both proteins in a population of cells. These studies revealed that both proteins undergo oscillatory behavior after DNA damage, but these oscillations appeared to be damped. An important breakthrough in the comprehension of this system was achieved a few years ago when researchers tracked, cell by cell the concentration of p53 and Mdm2 after irradiation with gamma rays [7, 8]. They found that, when looking into single cells, the oscillations are undamped, with a fixed frequency and a highly variable amplitude, suggesting that the previous reports of damped oscillations resulted from the average over the population of cells. More recent experiments of the same groups were fundamental to clarify the following issues [9–11]:

- The dynamics of p53 is dephased from the dynamics of Mdm2 and both are characterized by a fixed frequency and variable amplitudes of oscillations within a single cell.

- p53 is activated by a mechanism that leads to similar pulses in unstressed conditions as in response to DNA damage, but the pulses in unstressed conditions do not lead to cell cycle arrest or apoptosis.

- The study of the Fourier spectra of the oscillations has shown that the characteristic frequency of oscillation changes from $f \approx 0.14 h^{-1}$ when the system is under DNA damage to $f \approx 0.08 h^{-1}$ in basal conditions.

From the mathematical point of view these results inspired the development of new models. Most of them based on mean field equations with some biological motivated noise, added ad hoc, to stabilize the oscillations [9, 12, 13]. Alternatively, the oscillations may be stabilized introducing additional feedback-loops to the usual p53-Mdm2 model [14] or temporal delays [15].

Surprisingly, while it is well known that the number of p53 molecules in a single cell is small (around 10^3–10^4[16]), indicating that mean field approaches may not be appropriate approximations, only few previous studies [17–19] suggested that the finite size of the populations could be the source of the stability in the oscillations. However, most of these works considered only simulations and none of them compared in a quantitative manner the results of these simulations with experimental data. Here, we push this idea further, studying the isolated p53-Mdm2 module, but also the module in the presence of different external stresses: DNA damage and oncogenic response. In these two cases the role of the finite size fluctuations is studied for the first time. Moreover, we clarify, through analytic arguments, the role of the parameters of the models in the stability of the oscillations. With these predictions we went for the main goal of our work, to show that this mechanism may *quantitatively* explain, in different conditions, the experimental data of the p53-Mdm2 module dynamics in single cells.

The p53-Mdm2 model and Mathematical Background

Probably the simplest version, and the starting point of any development of the p53-Mdm2 module is the loop presented in figure 1. This is a feedback loop in which p53
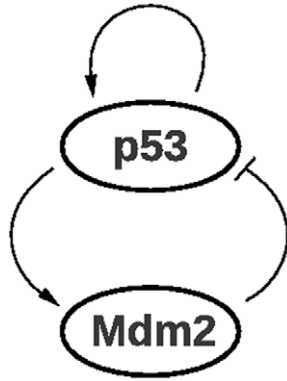
Figure 1. Sketch of the p53-Mdm2 feedback loop in its basal state. The protein p53 activates Mdm2 and Mdm2 suppresses p53.

acts as a transcription factor that regulates the expression of Mdm2 which, in turn, regulates the activity of p53. This is a well studied model [8, 9], whose mean field solution is characterized by damped oscillations. Sometimes, it is convenient to introduce in the model an intermediary species for the interaction between p53 and the Mdm2, usually a messenger mRNA that acts as the transcription factor of the Mdm2. We have shown before [19] that this intermediary is the responsible for the above mentioned dephasing between the oscillations of p53 and Mdm2 proteins. However, for simplicity we will assume here that it is in equilibrium, keeping the scheme of figure 1, as our basic block for the p53-Mdm2 module.

We formalize the model starting from a stochastic approach considering the number of components of each species, p53 (n_{p53}) and Mdm2 (n_{Mdm2}) as the relevant variables of the problem.

From this point of view one faces the problem of solving the following Master equation:

$$\frac{\partial P(\bar{n}, t)}{\partial t} = \sum_{\vec{n} \neq \vec{n'}} \left(P(\vec{n'}, t) \, W_{\vec{n'} \to \vec{n}} - P(\vec{n}, t) \, W_{\vec{n} \to \vec{n'}} \right) \tag{1}$$

where $P(\bar{n}, t)$ is the probability that the system is in state $\vec{n} = (n_{\mathrm{p53}}, n_{\mathrm{Mdm2}})$ at time t and $W_{\vec{n} \to \vec{n'}}$ are transition rates from one state to another. The solution of equation (1) is an easy task only for very simple transition rates and one must usually use numerical methods, or resort to approximations. In this work we try both approaches and compare the results.

The simulations of the temporal evolution of the system can be obtained using the Gillespie algorithm [20]. As other Monte Carlo techniques this algorithm guarantees an exact solution, but it is time consuming and is not a good tool to explore the parameter space. Moreover, to understand the role of the parameters of the model it is important to have at least approximate solutions to the problem. Here, we use the Linear Noise Approximation (LNA) [21], that was first proposed in the context of chemical kinetics and have gain considerable attention in the last few years for modeling intracellular processes, [22–24], but also in more general contexts [25, 26]. In addition we compare the results of this approximation with experimental data from the literature. The

mathematical details can be found in [21], and we summarize them in the appendix A for completeness. However, to simplify the reading, and to keep the consistency of the manuscript we present here its main results.

One of the difficulties to solve equation (1) is the discrete character of n_i. To deal with this, van Kampen [21] proposed the following approximation:

$$n_i = \Omega x_i + \sqrt{\Omega}\, \alpha_i \tag{2}$$

i.e. one approximates the number of *molecules* of species i by some concentration, plus some fluctuations proportional to the square root of the system size Ω. Substituting (2) into (1) and developing the equation in order of $\frac{1}{\Omega}$ one obtains, at first order a set of differential equations for x_i, usually called the mean field or deterministic approximation:

$$\frac{\partial x_i}{\partial \tau} = \sum_j S_{ij} \widehat{W}_j(\vec{x}\Omega) \tag{3}$$

where S_{ij} is the stoichiometric matrix of the interactions (see the appendix A) for a detail derivation). At second order one can prove that the fluctuations α_i are Gaussian variables. However, to compare them with the experiments it is more useful to describe the evolution of these variables in terms of Langevin equations.

$$\frac{\partial \alpha_i}{\partial \tau} = \sum_{k=1}^{N} A_{ik}\alpha_k + \eta_i(\tau) \tag{4}$$

where $A_{ik} = \sum_{j=1}^{M} S_{ik}\frac{\partial W_{ij}}{\partial x_k}$ and the η_i has zero variance and correlation function $\langle \eta_i(\tau)\eta_j(\tau') \rangle = D_{ik}\delta(\tau - \tau')$ with $D_{ik} = \sum_{j=1}^{M} S_{ij}S_{kj}W_j(\vec{x})$ (see the appendix A).

Equation (4) is a linear Langevin equation that can be easily solved in the Fourier representation

$$\hat{\alpha}_i(w) = \sum_k \Phi_{ik}^{-1}\hat{\eta}_k(w) \tag{5}$$

where $\Phi_{ik} = \mathrm{i}w\delta_{ik} - A_{ik}$. From $\hat{\alpha}_i(w)$ one can get the power spectrum of the fluctuations as:

$$P_i(w) = \langle |\alpha_i(w)|^2 \rangle = \sum_j \sum_k \Phi_{ij}^{-1}(\omega)D_{jk}(\Phi^*)_{ki}^{-1}(\omega) \tag{6}$$

which, when studying fluctuations in single cells, is the quantity usually reported experimentally [9].
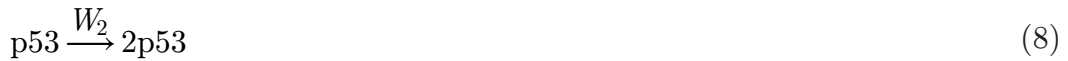
Results

In this section we present the main results of our work. It is divided in three parts, in each one of them the p53-Mdm2 module is studied either as an isolated structure or considering its interactions with different external elements. The organization of each

subsection is the same, we first motivate the model from the biological point of view and then present its stochastic formulation. We will show the results of simulations using Gillespie's algorithm and compare them with the prediction of the corresponding mean field solution (3). Then, we study the fluctuation spectra obtained from the simulations and compare them with the predictions of the Linear Noise Approximation (LNA). Finally we discuss the connection with experimental results in similar model systems.

Basal response

In the absence of any external signals p53, is activated only by random DNA damage. This is a common event during the cell life cycle. Spontaneous hydrolysis, collapsing replication forks and oxidative stress [27, 28], but also metabolic stress may produce p53 activation [5]. Within this context we study the basal response using the model in figure 1.

In stochastic terms the model is well described by the following set of expressions:

$$\text{p53} \xrightarrow{W_1} \text{p53} + \text{Mdm2} \tag{7}$$

$$\text{p53} \xrightarrow{W_2} 2\text{p53} \tag{8}$$

$$\text{p53} \xrightarrow{W_3} \Phi \tag{9}$$

$$\text{Mdm2} \xrightarrow{W_4} \Phi \tag{10}$$

$$\text{p53} + \text{Mdm2} \xrightarrow{W_5} \text{Mdm2} \tag{11}$$

where equations (7) and (8) reflect the activation of Mdm2 and the self-activation of p53. Equations (9) and (10) the decay of both species and equation (11) reflects the regulation of p53 by Mdm2. The species Φ reflects a *vacuum* state that is irrelevant in the analytical description of the problem, but is conveniently introduced to allow the free variation of the quantities of p53 and Mdm2 during the simulation keeping the system's size controlled [24]. The intuition is that if N is the total number of particles in the system, these are p53, Mdm2, and the number of molecules of the Φ species. In this sense, the dummy variable can be interpreted as the set of species in the cell that are connected with the process of interest, but not taken explicitly into account within the model.

The different W_i are transition probabilities proportional to the size of the system [21]. To fix concepts we work with the simplest possible transition probabilities, in this case:

$$W_1 = k_1 \Omega x_{\text{p53}} \tag{12}$$

$$W_2 = k_2 \Omega x_{\text{p53}} \tag{13}$$

$$W_3 = k_3 \Omega x_{\text{p53}} \tag{14}$$

$$W_4 = k_4 \Omega x_{\text{Mdm2}} \tag{15}$$

$$W_5 = k_5 \Omega x_{\text{p53}} x_{\text{Mdm2}} \tag{16}$$

The transitions $(W_{1,\,2})$, i.e. activation of Mdm2, and self-activation of p53 are proportional to the amount of p53 in the system. The degradation of Mdm2, (W_4) is proportional to the amount of Mdm2. The p53 is degraded following two mechanisms, a normal degradation (W_3) proportional to the quantity of p53 in the cell, and a Mdm2-mediated degradation (W_5), that is proportional to the quantities of p53 and of Mdm2. This is a clear simplification of the problem. However, one must first notice that non-linear approaches, although used with success in the modelling of gene regulatory networks are approximate expressions designed to describe a known biological phenomenology in systems governed by large populations, where the concept of 'concentration' is well defined [29, 30]. On the contrary we are dealing with problems where the number of molecules of the species involved is rather small, and therefore the concept itself of concentration is ill-defined. Of course, one could also write down transition rates that may reproduce in the proper limit of large number of molecules Hill-type functions, but it is not necessary true that this is a better assumption for small systems. Our linear hypothesis is nevertheless valid far from the saturation regime of the Hill function- that indeed is usually defined for very large concentrations. Therefore, following (3) the mean-field equations of this model read:

$$\frac{\mathrm{d}x_{\text{p53}}}{\mathrm{d}t} = k_2 x_{\text{p53}} - k_3 x_{\text{p53}} - k_5 x_{\text{p53}} x_{\text{Mdm2}} \tag{17}$$

$$\frac{\mathrm{d}x_{\text{Mdm2}}}{\mathrm{d}t} = k_1 x_{\text{p53}} - k_4 x_{\text{Mdm2}} \tag{18}$$

The fixed points of these equations are: $(0, 0)$ and $\left(\frac{k_4 k_2}{k_1 k_5}, \frac{k_2}{k_5} \right)$ where to simplify notation we considered $k_2' = k_2 - k_3$ and relabeled it as k_2. Then, the non trivial solution has biological sense only if the rate of activation of p53 is larger than its degradation rate $(k_2 > 0)$.

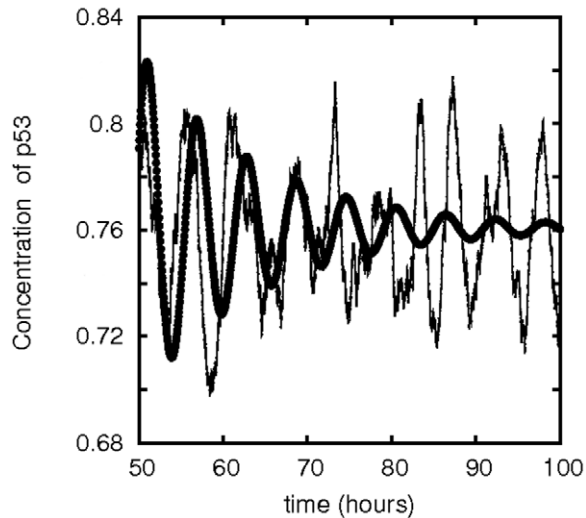The stability of these fixed points is defined by the following Lyapunov exponents:

$$(0, 0) \rightarrow \vec{\lambda} = \left\{ \begin{matrix} k_2 \\ -k_4 \end{matrix} \right\} \tag{19}$$

and:

$$(x_{\text{p53}}^*, x_{\text{Mdm2}}^*) \rightarrow \vec{\lambda} = \left\{ \begin{matrix} \dfrac{1}{2}\left(-k_4 + \sqrt{k_4^2 - 4k_2 k_4} \right) \\ \dfrac{1}{2}\left(-k_4 - \sqrt{k_4^2 - 4k_2 k_4} \right) \end{matrix} \right\} \tag{20}$$

These results guarantee that if the non-trivial solution exists ($k_4 > 0$ and $k_2 > 0$), then it is stable. Moreover, if $k_4 < 4k_2$, i.e. if the activation of p53 is large enough, it

Figure 2. Typical run showing the oscillations of p53 in the basal state. The bold curve indicates the mean field solution and the thin one are results from the Gillespie simulation. Parameters: $\vec{k} = (0.99, 1, 0.44, 0.49, 1.05)h^{-1}$.

displays damped oscillations. This is the region of parameters relevant from the biological point of view.

In figure 2 we show the comparison between the numerical solution of these equations with the results of the Gillespie algorithm for the same values of the parameters. Note that, while the deterministic solution is over-damped, the stochastic solution displays persistent oscillations around the fixed point.

To characterize these oscillations and in order to compare our model with the experimental results reported in [9], we computed the power spectrum of the results of the Gillespie simulations over 200 realizations and made their geometrical average. The resulting power spectrum of the oscillations of p53 extracted from the simulations is presented (symbols) in figure 3. In the same figure we also show (line) the analytical results predicted by the LNA (see equation (6) and the appendix A). The inset presents the tail of the power spectrum in a logarithmic scale. The linear dependency of this tail with the inverse of the frequency is also a prediction of the LNA.

The existence of a maximum in the power spectrum of the fluctuations in figure 3 is associated to the presence of a characteristic frequency for these fluctuations. In an infinite system, these oscillations die out, but the stochasticity due to the finite size of the system acts as a white noise, see equation (4), that interacts with the proper frequency of the system producing a resonance-like effect. This characteristic frequency is connected with the presence of an imaginary part in the eigenvalues of the system of differential equations and is a phenomena that has been very well characterized before in other models, see for example, [22–26]. In our specific case it is easy to show (see the appendix A), that the frequency of the oscillations only depends on the effective activation rate of p53 ($k_2 - k_3$) and the decay rate of Mdm2(k_4). On the contrary, the activation rate of Mdm2 by p53 (k_1) and the regulation of the p53 by Mdm2(k_5) although unavoidable to build the feed-back loop in the model are not connected with the characteristic frequency of the oscillations, suggesting a possible robust mechanism of interaction with other species.
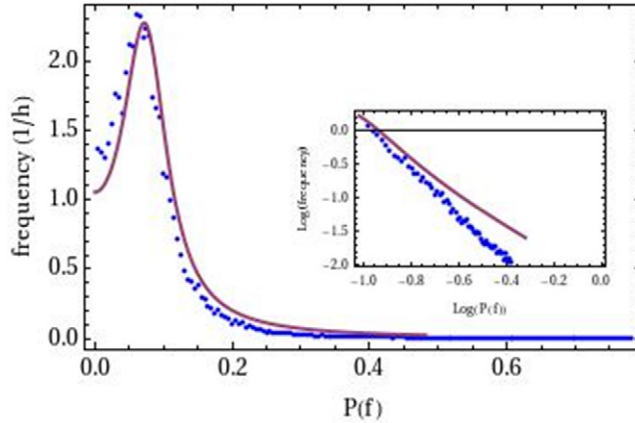
Figure 3. Average power spectrum of the fluctuations of p53 in its basal state. The points represent the power spectrum obtained after averaging over 1000 realizations of the Gillespie algorithm. The continue line is the prediction from the LNA. Note the existence of a characteristic frequency of oscillations. Parameters: $\vec{k} = (0.99, 1, 0.44, 0.49, 1.05)h^{-1}$.

The comparison with the experimental data is simplified with the help of the previous theoretical predictions that set a relation between some parameters of the model and the frequency of oscillations. This in turn can be extracted from the experimental data [9]. In this case for example we know (see the appendix A) that the frequency of oscillations is defined through the expression:

$$\omega = 2\pi f \approx \sqrt{(k_2 - k_3)k_4} \tag{21}$$

and from the experimental data [9] that $f = 0.08\ h^{-1}$, it is simply then to choose values of k_2, k_3 and k_4 that satisfy this condition and are consistent with previous predictions in the literature.

In fact, figure 3 compares also very well with figure 6 in [9] where the authors studied the basal response of the system and presented experimental results for the Fourier transform of the fluctuations. In that work the authors model their results adding some noise *ad-hoc* to mean field equations that are similar to ours. On the contrary, in our approach, the oscillations arise naturally from the finite size of the populations involved and reproduce very well the value reported in the experiments $f = 0.08\ h^{-1}$.

The rest of the parameters chosen have little influence in the main characteristic of the curve and as can be seen in the table 1 they compare very well with previous reports in the literature. Only k_5, the parameter reflecting the Mdm2-depending degradation rate of p53 is clearly underestimated in comparison with the value reported in [8]. But one must notice that, on one hand, their activation rate of p53 (k_2) is larger than ours, and on the other, that our model includes and Mdm2-independent degradation rate of p53 (k_3) that is absent in the model V of reference [8]. Therefore this underestimation of k_5 is not surprising at all.
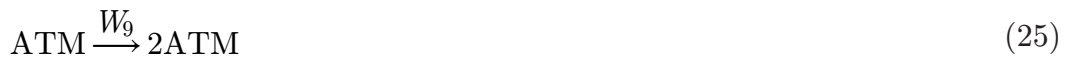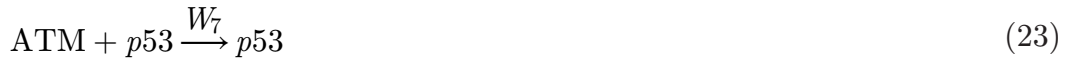
Response in the presence of stress

We already mentioned that p53 is one of the central proteins in the cellular response to stress. One of the most typical stresses is DNA double strand break (DSB), which could

Table 1. Comparison between our predictions for the values of the parameters of the model and similar estimates in the literature (Model V in [8]).

Parameter h^{-1}	This work	Literature
k_1	.99	1.5 ±60% [8]
k_2	1.0	2.0 ±25% [8]
k_3	0.44	—,— [8]
k_4	.49	0.9 ±30% [8]
k_5	1.05	3.7 ±50% [8]

be generated, for example, by gamma irradiation. The DSBs produces the activation of the upstream kinase ATM, that in turn induces the phosphorylation (activation) of p53. The p53, as already mentioned, then works as a transcription factor of several target genes. These genes activate different responses, ranging from DNA repair to apoptosis [10].

It is then natural, when modelling this kind of stress, to incorporate ATM as a new dynamical species. In figure 4 we present a sketch of this model. From the technical point of view, we must add to the dynamics governing the basal state the following new transitions:

$$\text{ATM} \xrightarrow{W_6} \text{ATM} + p53 \tag{22}$$

$$\text{ATM} + p53 \xrightarrow{W_7} p53 \tag{23}$$

$$\text{ATM} \xrightarrow{W_8} \Phi \tag{24}$$

$$\text{ATM} \xrightarrow{W_9} 2\text{ATM} \tag{25}$$

These transitions reflect the activation of p53 by the ATM, (W_6), the regulation of the ATM by p53, (W_7), the natural degradation of the ATM, (W_8), and a self-reinforcement field for the ATM, (W_9) that mimics the persistence of the damage. It is important however to take in mind that W_7 summarized a complex set of processes that after activation by p53 let to the DNA repair. As in the previous section we assumed that they take the following simple form:

$$W_6 = k_6 \Omega x_{\text{ATM}} \tag{26}$$

$$W_7 = k_7 \Omega x_{\text{p53}} x_{\text{ATM}} \tag{27}$$

$$W_8 = k_8 \Omega x_{\text{ATM}} \tag{28}$$

$$W_9 = k_9 \Omega x_{\text{ATM}} \tag{29}$$
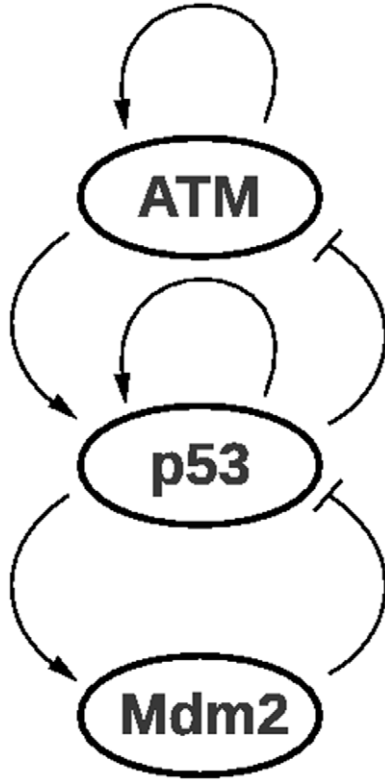
Figure 4. Sketch of the p53-Mdm2 feedback loop in the presence of DNA damage. The protein p53 activates Mdm2 and Mdm2 suppresses p53. Moreover. the ATM activates the p53 that in turn regulates ATM.

With these definitions of the transition rules, we may write the mean field equations of the model:

$$\frac{\mathrm{d}x_{\mathrm{p53}}}{\mathrm{d}t} = k_2 x_{\mathrm{p53}} - k_3 x_{\mathrm{p53}}$$
$$- k_5 x_{\mathrm{p53}} x_{\mathrm{Mdm2}} + k_6 x_{\mathrm{ATM}}$$
$$\frac{\mathrm{d}x_{\mathrm{Mdm2}}}{\mathrm{d}t} = k_1 x_{\mathrm{p53}} - k_4 x_{\mathrm{Mdm2}}$$
$$\frac{\mathrm{d}x_{\mathrm{ATM}}}{\mathrm{d}t} = k_9 x_{\mathrm{ATM}} - k_8 x_{\mathrm{ATM}} - k_7 x_{\mathrm{ATM}} x_{\mathrm{p53}} \tag{30}$$

These equations are similar to the ones in (18), but now the role of ATM on the activation of p53 results in the addition of a new term to the first equation. Moreover, ATM is also a new dynamical variable whose evolution must be taken into account.

This system of equations has three different fixed points. They are, $(0,0,0), \left(\frac{k_2 k_4}{k_1 k_5}, \frac{k_2}{k_4}, 0\right)$ and $\left(\frac{k_9}{k_7}, \frac{k_9 k_1}{k_7 k_4}, \frac{k_9}{k_7 k_6}\left(\frac{k_9 k_1 k_5}{k_7 k_4} - k_2\right)\right)$ where for simplicity we re-labelled again $k_2' = k_2 - k_3$, and $k_9' = k_9 - k_8$, as k_2 and k_9 respectively.

The Jacobian matrix necessary to study their stability takes the general form:

$$J = \begin{bmatrix} k_2 - k_5 x^*_{\text{Mdm2}} & -k_5 x^*_{\text{p53}} & k_7 \\ k_1 & -k_4 & 0 \\ -k_7 x^*_{\text{ATM}} & 0 & 0 \end{bmatrix}$$

that evaluated in the fixed point of interest $\left(\frac{k_9}{k_7}, \frac{k_9 k_1}{k_7 k_4}, \frac{k_9}{k_7 k_6} \left(\frac{k_9 k_1 k_5}{k_7 k_4} - k_2 \right) \right)$ transforms into the following secular equation:

$$\lambda^3 + \lambda^2 (c - k_4) + \lambda \left(\frac{k_9 k_1 k_5}{k_7} - k_4 c - k_9 c \right) - k_9 k_4 c = 0 \tag{31}$$

where $c = k_2 - \frac{k_9 k_1 k_5}{k_7 k_4}$.

This secular equation must be studied numerically and its solution defines the stability of the fixed points. We have found that depending on the parameters, three different regions are well defined. In Region I the solution $\{x^*_{\text{p53}}, x^*_{\text{Mdm2}}, x^*_{\text{ATM}}\}$ may exist, is stable and the system reaches the fixed point with damped oscillations. In this region also the solution $\{x^*_{\text{p53}}, x^*_{\text{Mdm2}}, 0\}$ is stable if $k_2 > 0$. Depending on the initial condition, the system is attracted to one or another fixed point. In Region II the solution $\{x^*_{\text{p53}}, x^*_{\text{Mdm2}}, x^*_{\text{ATM}}\}$ has biological sense and is stable, but the fixed point is reached without damped oscillations. In this region the solution $\{x^*_{\text{p53}}, x^*_{\text{Mdm2}}, 0\}$ does not exist. Finally, in Region III only the solution $\{x^*_{\text{p53}}, x^*_{\text{Mdm2}}, 0\}$ is stable.

Based on the results of the previous section we concentrate our attention in Region I, where the mean field fixed point $\{x^*_{\text{p53}}, x^*_{\text{Mdm2}}, x^*_{\text{ATM}}\}$ is reached quickly through over-damped oscillations. In figure 5 we show the numerical solution of equation (29) and the results of the Gillespie algorithm using the parameters $\vec{k} = (0.99, 1, 0.44, 0.69, 0.85, 0.5, 0.5, 0.1, 0.4) h^{-1}$. In the left panel of the figure we plot the first 30 h of the simulations, and compare them with the mean-field solutions. It is clear that while the over-damped oscillations die out very fast, the stochastic fluctuations are sustained by a large period of time. This is represented in the right panel in the same figure where these fluctuations are shown for up to 110 h.

To characterize these oscillations we use again the power spectrum of the Gillespie results and compare them with the predictions from the LNA. In figure 6 we show with points this power spectrum and with a continuous line the predictions from the LNA. As in the previous section, in the inset we plot the tail power spectrum in a logarithmic scale, showing again a linear dependency with $1/\omega$. Notice the good coincidence between the numerical simulations and the LNA.

We may also compare our results with figure 3 in [9]. Again, our model may reproduce qualitatively and quantitatively the experimental observations: the existence of a characteristic frequency ($f = 0.14~h^{-1}$), compatible with the experimental results and larger that in the basal state, and a divergence close to zero frequency. The parameters were intentionally chosen to resemble the experiments. As before, the characteristic frequency of the oscillations is essentially defined by $k_2 - k_3$ and k_4. We fit the expected experimental frequency ($f = .14~h^{-1}$) [9], increasing (decreasing) k_4 (k_5) with respect to the model in the basal state to resemble the experimentally verified fact that under DNA damage the degradation rate of Mdm2 increases and the Mdm2-mediated
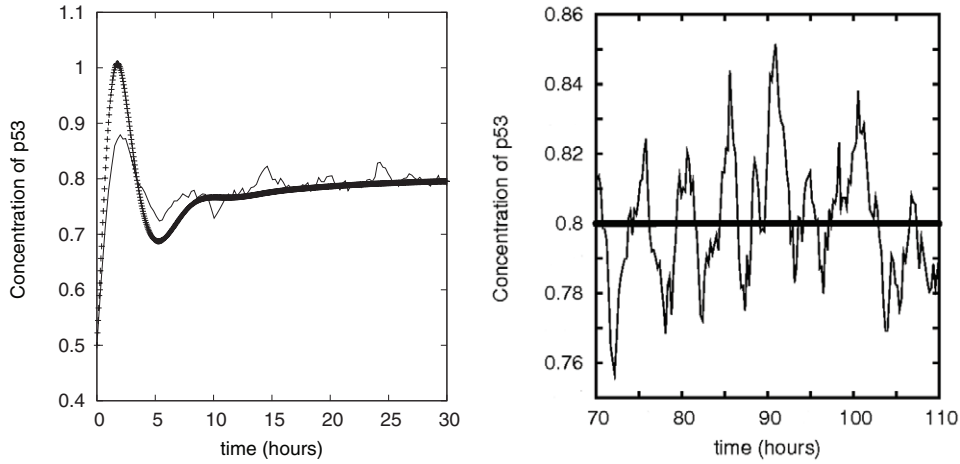
Figure 5. Typical run showing the oscillations of p53 in the presence of DNA damage. Left panel: The first hours of oscillations. It should be notice the fast damping predicted by the mean-field model. Right panel: Long time dynamics. The bold curve indicates the mean field solution and the thin one are results from the Gillespie simulation. Parameters: $\vec{k} = (0.99, 1, 0.44, 0.69, 0.85, 1.5, 1.5, 0.1, 1.0)h^{-1}$.
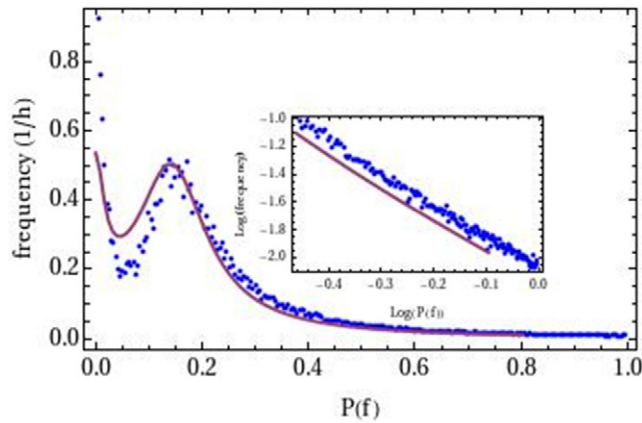
Figure 6. The points represent the power spectrum obtained after averaging over 200 realizations of the Gillespie algorithm. The continue line is the prediction from the LNA. Note the existence of a characteristic frequency of oscillations and a divergence close to zero frequency. Parameters: $\vec{k} = (0.99, 1, 0.44, 0.69, 0.85, 1.5, 1.5, 0.1, 1.0)h^{-1}$.

degradation rate of p53 decreases [31]. Moreover, to reproduce the divergence at low frequency of the model we noticed that it is associated with the parameters characterizing the new feed-back loop. It can be interpreted looking to the low frequency analytical expression of the power spectrum derived from the LNA. It has the non-trivial form:

$$P_{\text{p53}}(w \to 0) \sim \frac{2k_5 k_7}{k_1 k_6 k_8 - k_2 k_5 k_7} \qquad (32)$$

that nonetheless guarantees, if the denominator is small enough, a large value for the power spectrum. With this expression, the numerical results of the previous section and

13

Table 2. Comparison between our predictions for the values of the parameters of the model and similar estimates in the literature, Model VI in [8] and a cross-regulated linear model in [9].
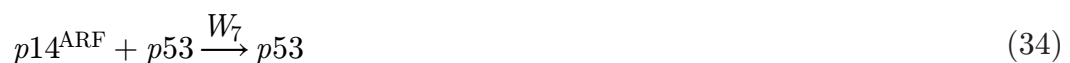
Parameter h^{-1}	This work	Literature
k_1	0.99	$0.29 \pm .03\%$ [9], 1.20 [8]
k_2	1	$2 \pm .5\%$ [9], 0.8 [8]
k_3	.44	$.45 \pm .03\%$ [9], $1.40 \pm 20\%$ [8]
k_4	.69	$.28 \pm .02\%$ [9]
k_5	.85	$.55 \pm .05\%$ [9]
k_6	.5	$k_6 k_7 = .65 \pm .05\%$ [9]
k_7	.5	$k_6 k_7 = .65 \pm .05\%$ [9]
k_8	.4	

previous estimates from the literature, it was easy to choose values for the parameters that reproduce the divergence of the experimental data and the correct frequency of resonance (see table 2). However, we want to stress that there is still a lot of freedom in the parameter selection and our interest here was not to find the best ones, but just to show that this approach provides a straightforward path to obtain a quantitative comparison between our theoretical model and the experimental data. It must be noticed that excluding the parameters that were fixed to reproduce the divergence at low frequency and the peak in the power spectrum, variations within a 10% of the values reported in table 2 reproduce curves qualitatively similar to figure 6. All these values compare very well with previous theoretical estimates of equivalent parameters in similar models, as presented also in table 2.
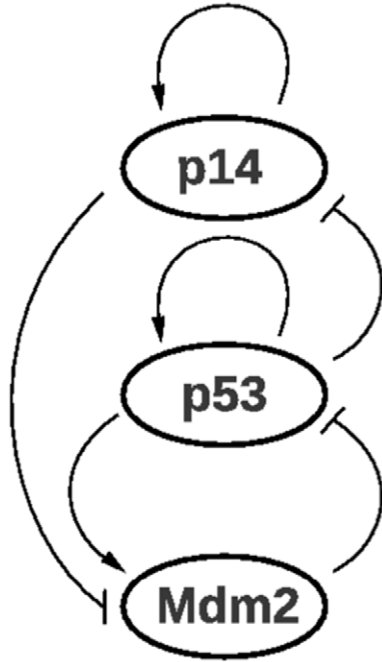
Oncogenic response

Another important pathway for the activation of p53, comes from the activation of the p14$^{\mathrm{ARF}}$ protein. In the presence of oncogenes this protein is activated and joins Mdm2 accelerating its degradation [32]. This process leads to the increase of p53 level in the cell. Unfortunately, as far as we know there is no experimental evidence for the single cell dynamics of p53 and Mdm2 in the presence of oncogenes, therefore some of the parameters used in this section lack of experimental bias. Nevertheless we will show that independently of the values used, the power spectrum of the fluctuations is qualitatively different from the one obtained when p53 interacts directly with ATM.

The model of oncogenic response is sketched in figure 7. To the standard interactions present in the basal model we add the regulation of p14$^{\mathrm{ARF}}$ to Mdm2 and a regulation of p14$^{\mathrm{ARF}}$ by p53. In terms of stochastic transitions we have now:

$$\mathrm{Mdm2} + p14^{\mathrm{ARF}} \xrightarrow{W_6} p14^{\mathrm{ARF}} \tag{33}$$

$$p14^{\mathrm{ARF}} + p53 \xrightarrow{W_7} p53 \tag{34}$$

$$p14^{\mathrm{ARF}} \xrightarrow{W_8} \Phi \tag{35}$$

Figure 7. Sketch of the p53-Mdm2 feedback loop in the presence of DNA damage. The protein p53 activates Mdm2 and Mdm2 suppresses p53. Moreover. the ATM activates p53 that in turn regulates ATM.

$$p14^{\text{ARF}} \xrightarrow{W_9} 2p14^{\text{ARF}} \tag{36}$$

and defining the transition rates as:

$$W_6 = k_6 \Omega x_{\text{p14}} x_{\text{Mdm2}} \tag{37}$$

$$W_7 = k_7 \Omega x_{\text{p53}} x_{\text{p14}} \tag{38}$$

$$W_8 = k_8 \Omega x_{\text{p14}} \tag{39}$$

$$W_9 = k_9 \Omega x_{\text{p14}} \tag{40}$$

we obtain the following system of equations for the dynamic of the model:

$$
\begin{aligned}
\frac{\mathrm{d}x_{\text{p53}}}{\mathrm{d}t} &= k_2 x_{\text{p53}} - k_3 x_{\text{p53}} - k_5 x_{\text{p53}} x_{\text{Mdm2}} \\
\frac{\mathrm{d}x_{\text{Mdm2}}}{\mathrm{d}t} &= k_1 x_{\text{p53}} - k_4 x_{\text{Mdm2}} - k_6 x_{\text{p14}} x_{\text{Mdm2}} \\
\frac{\mathrm{d}x_{\text{p14}}}{\mathrm{d}t} &= k_9 x_{\text{p14}} - k_8 x_{\text{p14}} - k_7 x_{\text{p14}} x_{\text{p53}}
\end{aligned}
\tag{41}
$$
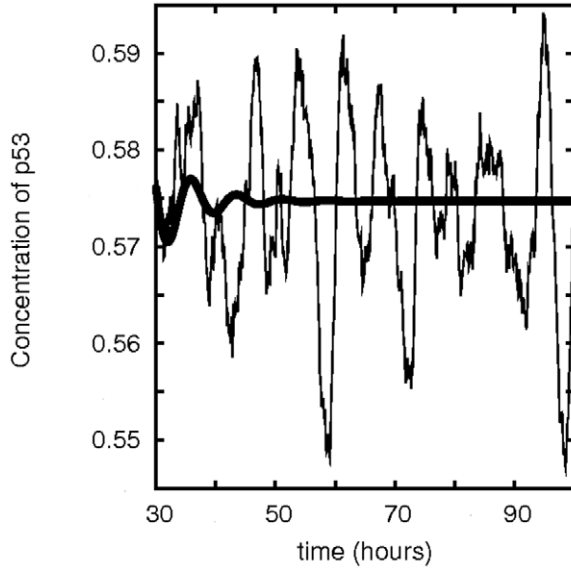
Figure 8. Typical run showing the oscillations of p53 in the presence of oncogenic signals. The bold curve indicates the mean field solution and the thin one are results from the Gillespie simulation. Parameters: $\vec{k} = (1.0, 1.0, 0.44, 0.69, 0.85, 0.5, 0.5, 0.4)$.

which again depending on the parameters may show three fixed points: $(0, 0, 0)$, $\left(\frac{k_2 k_4}{k_1 k_5}, \frac{k_1}{k_5}, 0\right)$ and $\left(\frac{k_9}{k_7}, \frac{k_2}{k_5}, \frac{1}{k_2 k_6}\left(\frac{k_9 k_1 k_5}{k_7} - k_2 k_4\right)\right)$. To simplify the notation we have used $k_2 = k_2 - k_3$ and $k_9 = k_9 - k_7$.

The Jacobian matrix near these fixed points takes the form:

$$J = \begin{bmatrix} k_2 - k_5 x^*_{\text{Mdm2}} & -k_5 x^*_{\text{p53}} & 0 \\ k_1 & -k_4 & -k_6 x^*_{\text{Mdm2}} \\ -k_2 x^*_{\text{p14}} & 0 & k_9 \end{bmatrix} \tag{42}$$

that evaluated in the fixed point $\{x^*_{\text{p53}}, x^*_{\text{Mdm2}}, x^*_{\text{p14}}\}$ leads to the following secular equation:

$$\lambda^3 + \lambda^2 k_4 + \lambda\left(\frac{k_9 k_1 k_5}{k_7}\right) + \frac{k_9^2 k_5 k_1}{k_7} - k_2 k_9 k_4 = 0 \tag{43}$$

which defines a phase diagram qualitatively similar to the one discussed in the preceding section. Three regions, but only one of them, with solution $\{x^*_{\text{p53}}, x^*_{\text{Mdm2}}, x^*_{\text{p14}}\} \neq \vec{0}$ displays damped oscillations. Our previous results suggest that this is the relevant region for our purposes. In this region we used $\vec{k} = (1.0, 1.0, 0.44, 0.69, 0.85, 0.5, 0.5, 0.4)$ as parameters to obtain damped oscillations in the mean field solution of the problem and sustained oscillations through the Gillespie algorithm. The results are shown in figure 8.

In figure 9 we show the power spectrum obtained using the LNA and the one obtained from the simulations. Also for this model, the LNA approximation correctly describes the results of the simulation. As before a clear peak representative of the
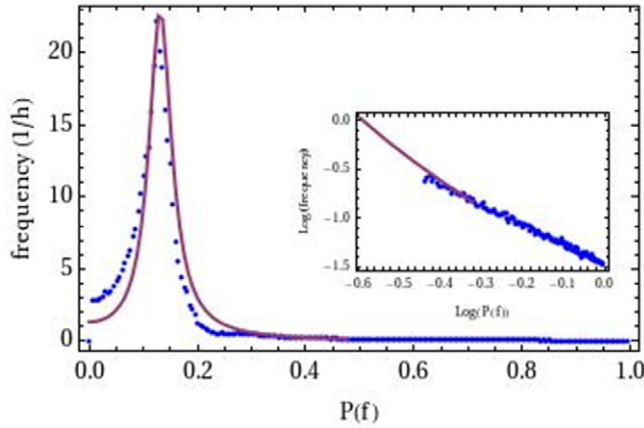
Figure 9. The points represent the power spectrum obtained after averaging over 200 realizations of the Gillespie algorithm. The continue line is the prediction from the LNA. Note the existence of a characteristic frequency of oscillations and a divergence close to zero frequency. Parameters: $\vec{k} = (1.0, 1.0, 0.44, 0.69, 0.85, 0.5, 0.5, 0.4)$.

feed-back loop between p53 and Mdm2 is observed and also the exponential decay of the tail of the power spectrum with $1/\omega$. However, there is no evidence of a divergence at small frequencies.

This absence of the divergence is independent of the parameters chosen. It can be understood looking again to the structure of the power spectrum predicted by the LNA at small frequencies. For this model:

$$P_{\text{p53}}(w \to 0) = \frac{2k_5(k_1 + k_2)}{k_1^2 k_6} \tag{44}$$

that indicates that only when k_1 or k_6 are zero, i.e. only when the regulation of Mdm2 by p53 or the interaction between Mdm2 and p14$^{\text{ARF}}$ disappears we have a diverging power spectrum at small frequencies. But in this case our model of interactions breaks down.

Discussion

The fact that noise is part of cellular systems has been known for many years. Noise, however may come from many sources and it is not a simple procedure to unveil which is the relevant one in a specific process. In cell populations the randomness is usually hidden in the average measurement making hard, if not impossible, to trace back the main source of stochasticity. But also results from single cell measurements should be interpreted with great care. External sources of noise are always present, for example when irradiating a population of cells one can never guarantee which one was really affected and how much, but even within the same culture, cells sense different local environments responding differently to apparently similar external conditions. Protein degradation and production rates, which in biology are processes usually parametrized with one number each, may vary, from cell to cell, but also within each cell in different conditions. Moreover, when

the processes of interest involve a small number of molecules, also the stochasticity due to small size fluctuations may become relevant. Then, the only way to choose among the different alternatives is to build model systems and to compare its possible outputs with experimental data. In this section we first introduce some previous approaches to the problem that may be helpful to put our work in context and then discuss our results.

As already explained in the introduction the p53-Mdm2 module has been the subject of many theoretical and experimental studies, but it was not until the single cells experiments developed in the last few years [7–10] that the presence of sustained oscillations were considered as a relevant phenomena in this system.

Early attempts to describe these oscillations essentially generalized known mean-field descriptions of the module dynamics. For example in the work of Tiana *et al* [15] the authors considered simple mean-field equations for the concentration of the proteins but assumed a time delay in the interaction between p53 and the Mdm2, this time delay was associated to the transcription process of the Mdm2. Following a completely different perspective Elias *et al* [33] considered the module in the presence of another protein, Wip1, that is also regulated by p53. In addition, both negative feed-back loops, p53-Mdm2 and p53-Wip1, belong to different interacting compartments of the cell. Within the same spirit , in reference [34], the authors extend the basic p53-Mdm2 model with new equations differentiating p53 and Mdm2 inside and outside the cellular nucleus and took into account the effect of the irradiation in the DNA damage. A more sophisticated road was followed in reference [35], where the authors developed a completed spatio-temporal model in which the diffusion of the molecules in the cell is taken into account through partial differential equations. In all these cases the models sustain the oscillations of p53 and the Mdm2, and their dephasing, but fail to predict the heterogeneity in the dynamical responses within single cell experiments, for example, the differences in amplitudes of the oscillations from cell to cell, or in time within a given cell. To account for these effects within these kind of models one must add, ad hoc, some sort of stochasticity in the parameters of the models.

This was the approach followed in references [13, 36] and by Zatorsky and collaborators in [8, 9] where the authors analyzed several stochastic models inspired in previous mean field descriptions trying to reproduce their own experimental data. Their results suggest that the low frequency noise (6–12 h) in the production rates of the proteins is a good candidate to explain the experimental data. Moreover, the best results are obtained for a model that includes a delay in the translation of Mdm2(in the same spirit of Tiana *et al* [15]). However this approach suffers from the lack of a formal justification. It starts with the assumption that the macroscopic equations describing the dynamics of p53-Mdm2 module are correct and then introduce a biologically motivated noise. As we already discussed the first assumption is valid only when the number of molecules involved is large. But also the ad hoc introduction of a noise in equations for macroscopic variables is usually not mathematically justified and may produce unwanted errors. To introduce the noise one must consider all the relevant long time correlations within the macroscopic equations of the problem, and this is certainly not the case here, (see [37] for an accurate discussion on this issue).

Alternatively and as previously mentioned the role of finite size fluctuations were also considered to explain the dynamics of the p53-Mdm2 module [17–19]. Already in reference [25] it was clear that these kind of fluctuations could produce resonance-like

effects in similar models. The rationale behind the phenomena is well established, the white noise induced by finite-size fluctuations resonates with the characteristic frequency of the system. Our results are in line with these previous predictions They feed the intuition that, provided that it resonates with the characteristic frequency of the feed-back loop, *any source of noise* is sufficient to sustain oscillations over long times.

However, in addition our results provide (as far as we know) the first *quantitative comparison* between real biological experiments and a model where finite size fluctuations are the one responsible of sustained oscillations. This comparison is strengthen here by two facts. First, the main properties of the experimental data i.e. the characteristic frequencies of the oscillations and the divergence of the power spectrum in the presence of damage are fixed, within the Linear Noise Approximation, through analytical relations that set the range of parameter values allowed. This is something absent in previous approaches [17, 18]. Second, the actual values of the parameters used to fit the data are biologically reasonable and compare very well with previous experimental and numerical values in the literature. Moreover, we have already shown in [19] that the introduction of an intermediary for the transcription of Mdm2 acts, within this finite size approximation, as a *a mechanism that delays the production of Mdm2*, producing a dephasing between the oscillations of p53 and the Mdm2, in the same spirit of [8, 15, 33]. All these results support the idea that finite size fluctuations are a plausible mechanism to be responsible of the sustained oscillations in the p53-Mdm2 module. Further experimental tests may help to solidify this. For example, a straightforward conclusion of our analysis is that, independently of the model, the frequency of the oscillations depends only on the production rate of p53 and the degradation rate of Mdm2, it could be interesting to design new experimental protocols to test this prediction.

Conclusions

We studied, using analytical tools (LNA) and numerical simulations (Gillespie's algorithm) the p53-Mdm2 module in its basal state, in the presence of DNA damage and of oncogenic signals. The module is studied as a stochastic system where finite size effects are relevant and responsible of the fluctuations in the number of molecules. Our model *quantitatively* reproduces the experimental values for the frequency of the oscillations in the basal state and in the presence of stress. The approach also explains the sharp increase at low frequency of the power spectrum of the fluctuations in the presence of stress, allowing a clear connection between these results and the parameters of the model. Moreover, it is easily extensible to reflect also the dephasing between the oscillations of Mdm2 and p53 proteins. Our results suggest that the intrinsic noise due to the finite size of the populations of p53 and Mdm2 is the main responsible of the sustained oscillations in the response of the p53-Mdm2 circuit.

Acknowledgments

Authors contributions

Appendix A

A.1. Linear Noise Approximation

The quantities characterizing the number of particles in our problem are discrete. The deviation of this number from the expected mean value produces fluctuations usually called *intrinsic noise* because it is not caused by any external source. When the system is small enough, this intrinsic noise is not negligible, and a mean field approximation can not be taken.

In these cases, the correct way to describe the system is to solve the Master Equation that governs it:

$$\frac{\partial P(\bar{n}, t)}{\partial t} = \sum_{\vec{n} \neq \vec{n'}} \left(P(\vec{n'}, t) \, W_{\vec{n'} \to \vec{n}} - P(\vec{n}, t) \, W_{\vec{n} \to \vec{n'}} \right). \tag{A.1}$$

This is an equation for the change in time of the probability $P(\vec{n}, t)$ of being in the state $\vec{n}$ at the time t, and it rests upon the Markovian hypothesis. $W_{\vec{n} \to \vec{n'}}$ are transition rates from states $\vec{n}$ to $\vec{n'}$.

An important difficulty in solving the Master equation arises from the discreteness of the variables involved ($\vec{n}$). Its solution is obtained by analytical methods in very lucky situations. An approximation scheme that allows to get some information from it, is the linear noise approximation (LNA).

This approximation assumes the possibility of studying the number n_i of integrands of the ith population as a main part Ωx_i that represents the mean value of the population size, plus a small deviation $\sqrt{\Omega}\,\alpha_i$ that represents the fluctuations around the mean value, and that is proportional to the square root of the system size Ω. In this way:

$$n_i = \Omega x_i + \sqrt{\Omega}\,\alpha_i. \tag{A.2}$$

As every process that takes place in the system causes variations of one or more integrands in the populations of the species involved, it is useful to write the master equation in terms of these discrete fluctuations. For this purpose let us define the *step operator* as:

$$E_i^k f(\dots, n_i, \dots) = f(\dots, n_i + k, \dots). \tag{A.3}$$

In terms of this operator the master equation reads:

$$\frac{\mathrm{d}P(\vec{n}, t)}{\mathrm{d}t} = \sum_{j=1}^{M} \left[\left(\prod_{i=1}^{N} E_i^{-S_{ij}} \right) - 1 \right] W_j(\vec{n}, \Omega) P(\vec{n}, t), \tag{A.4}$$

where W_j is the microscopic reaction rate for the jth process and S_{ij} is the element (i, j) of the stoichiometry matrix $\mathbf{S}$, the magnitude of the change in the ith population when the jth process takes place. The total number of different populations that form the system is N, and M is the total number of different kinds of processes that can take place in the system.

In terms of the fluctuations, which are continuous variables, the step operator takes the following form, more suitable for an analytic treatment

$$E_i{}^k \approx 1 + \frac{k}{\sqrt{\Omega}}\frac{\partial}{\partial\alpha_i} + \frac{k^2}{2\Omega}\frac{\partial^2}{\partial\alpha_i{}^2} + \ldots \tag{A.5}$$

in this way, we can work with a continuous operator, and still not lose the stochastic features of these processes. With it

$$\prod_{i=1}^{N} E_i^{-S_{ij}}f_j(\vec{\alpha},\Omega) = \left[1 - \Omega^{-\frac{1}{2}}\sum_{i=1}^{N}S_{ij}\frac{\partial}{\partial\alpha_i}\right]f_j(\vec{\alpha},\Omega)$$
$$+ \frac{1}{2}\left[\Omega^{-1}\sum_{i=1}^{N}\sum_{k=1}^{N}S_{ij}S_{kj}\frac{\partial}{\partial\alpha_i}\frac{\partial}{\partial\alpha_k} + \ldots\right]f_j(\vec{\alpha},\Omega) \tag{A.6}$$

Now we are going to replace the probability $P(\vec{n},t)$ by the probability $\Pi(\vec{\alpha},t)$ of being $\sqrt{\Omega}\,\vec{\alpha}$ away from the mean field prediction

$$P(\vec{n},t) = P\left(\Omega\vec{x} + \sqrt{\Omega}\,\vec{\alpha}\right) = \Pi(\vec{\alpha},t) \tag{A.7}$$

We know that:

$$\frac{\partial\Pi(\vec{\alpha},t)}{\partial t} = \frac{\partial P(\vec{n},t)}{\partial t} + \Omega\sum_{i=1}^{N}\frac{\partial P(\vec{n},t)}{\partial n_i}\frac{\partial x_i}{\partial t} \qquad \text{and}$$
$$\frac{\partial P(\vec{n},t)}{\partial n_i} = \frac{1}{\sqrt{\Omega}}\frac{\partial\Pi(\vec{\alpha},t)}{\partial\alpha_i},$$

with this results we can obtain the relation

$$\frac{\partial\Pi(\vec{\alpha},t)}{\partial t} - \Omega^{\frac{1}{2}}\sum_{i=1}^{N}\frac{\partial\Pi(\vec{\alpha},t)}{\partial\alpha_i}\frac{\partial x_i}{\partial t} = \frac{\partial P(\vec{n},t)}{\partial t}. \tag{A.8}$$

If now we expand the transition probabilities per unit time around $\vec{x}$

$$W_j(\vec{\alpha},\Omega) = W_j\left(\vec{x} + \Omega^{-\frac{1}{2}}\vec{\alpha}\right) \simeq W_j(\vec{x})$$
$$+ \Omega^{-\frac{1}{2}}\sum_{i=1}^{N}\frac{\partial W_j(\vec{x})}{\partial x_i}\alpha_i + o(\Omega^{-1}) \tag{A.9}$$

Substituting (A.6) and (A.9) in the master equation (A.4) and using (A.7), after grouping the coefficients of the similar powers of Ω we find:

$$\frac{\partial P(\vec{n}, t)}{\partial t} = \Omega^{-1} \left(\sum_{j=1}^{M} W_j(\vec{x}) \sum_{i,k=1}^{N} S_{ij} S_{kj} \frac{\partial^2 \Pi(\vec{\alpha}, t)}{\partial \alpha_i \partial \alpha_k} \right)$$

$$- \Omega^{-1} \left(\sum_{j=1}^{M} \sum_{i,k=1}^{N} S_{ij} \frac{\partial [\Pi(\vec{\alpha}, t) \alpha_k]}{\partial \alpha_i} \frac{\partial W_j(\vec{x})}{\partial x_k} \right)$$

$$+ \Omega^{-\frac{1}{2}} \left(- \sum_{j=1}^{M} \sum_{i=1}^{N} S_{ij} W_j(\vec{x}) \frac{\partial \Pi(\vec{\alpha}, t)}{\partial \alpha_i} \right) + o\left(\Omega^{-\frac{3}{2}} \right)$$

If now we compare the coefficients of the similar powers of Ω in equations (A.10) and (A.8), where the unit of time has been changed from t to $\tau = \frac{t}{\Omega}$ we find for the leading order:

$$\frac{\partial x_i}{\partial \tau} = \sum_{j=1}^{M} S_{ij} W_j(\vec{x}). \tag{A.10}$$

This corresponds to the deterministic rate equations that are often used to describe the dynamics of such systems at a mean-field level. It has been discussed already in the subsection referring to mean field equations and stability analysis.

For the coefficients of Ω^{-1} the relation reads:

$$\frac{\partial \Pi(\alpha, \tau)}{\partial \tau} = - \sum_{i,k=1}^{N} A_{ik} \frac{\partial [\Pi(\alpha, t) \alpha_k]}{\partial \alpha_i}$$

$$+ \frac{1}{2} \sum_{i,k=1}^{N} D_{ik} \frac{\partial^2 \Pi(\alpha, t)}{\partial \alpha_i \partial \alpha_k}, \tag{A.11}$$

where

$$A_{ik} = \sum_{j=1}^{M} S_{ij} \frac{\partial W_j(\vec{x})}{\partial x_k} \tag{A.12}$$

is the jacobian matrix of the system, and

$$D_{ik} = \sum_{j=1}^{M} S_{ij} S_{kj} W_j(\vec{x}). \tag{A.13}$$

Equation (A.11) is a Fokker-Plank equation for the probability for the system to have the deviation $\sqrt{\Omega} \, \vec{\alpha}$ around the mean-field prediction. This equation can be written in a completely equivalent formulation more benevolent to investigation using Fourier transforms. The problem can then be formulated as the set of stochastic differential equations of the Langevin type:

$$\frac{\mathrm{d}\alpha_i}{\mathrm{d}\tau} = \sum_{k=1}^{N} A_{ik} \alpha_k + \eta_i(t) \tag{A.14}$$

where $\eta_i(\tau)$ is a Gaussian noise with 0 mean and correlation given by $\langle \eta_i(\tau) \eta_k(\tau') \rangle = D_{ik} \delta(\tau - \tau')$.

This a linear Langevin equation that can be easily solved in the Fourier representation

$$\hat{\alpha}_i(w) = \sum_k \Phi_{ik}^{-1} \hat{\eta}_k(w) \tag{A.15}$$

where $\Phi_{ik} = iw\delta_{ik} - A_{ik}$. From $\hat{\alpha}_i(w)$ one can get the the power spectrum of the fluctuations as:

$$P_i(w) = \langle |\tilde{\alpha}_i(w)|^2 \rangle = \sum_j \sum_k \Phi_{ij}^{-1*} \Phi_{ik}^{-1} D_{jk} \tag{A.16}$$

A.2. Power spectrum in the basal state

Now we are going to analyze the general expression for the power spectrum (A.16) for the basal state. The analytics for the other two models develops following the same steps, with a more cumbersome Algebra

$$P_i(\omega) \propto \sum_{j=1}^N \sum_{k=1}^N \Phi_{ij}^{-1}(\omega) D_{jk} (\Phi^\dagger)_{ki}^{-1}(\omega) \tag{A.17}$$

Since $\Phi = i\omega\delta_{ik} - A_{ik}$ and since A and D are independent of ω, $P_i(\omega)$ is a fraction, the numerator and the denominator have both a polynomial structure of order $2N$. The explicit form of the denominator is: $|\det\Phi(\omega)|^2$.

Then, we expect that the enhancement of the fluctuations would be in the values of ω that minimize the denominator. Now we are going to analyze the general expression for the denominator of the power spectrum, and show explicit expressions for the basal response.

The matrix A in the expression of Φ is the jacobian matrix which can be written in terms of the eingenvalues, then we can write:

$$\begin{aligned}
\det\Phi(\omega) &= \det\begin{pmatrix} i\omega - \lambda_1 & 0 \\ 0 & i\omega - \lambda_2 \end{pmatrix} \\
&= -\omega^2 - i\omega(\lambda_1 + \lambda_2) + \lambda_1\lambda_2
\end{aligned} \tag{A.18}$$

$$\begin{aligned}
P_i(\omega) &\propto \frac{1}{(-\omega^2 - i\omega(\lambda_1 + \lambda_2) + \lambda_1\lambda_2)} \\
&= \frac{1}{(-\omega^2 + i\omega(\lambda_1 + \lambda_2) + \lambda_1\lambda_2)}
\end{aligned} \tag{A.19}$$

$$\begin{aligned}
P_i(\omega) &\propto \frac{1}{(\omega^2 - \lambda_1\lambda_2)^2 + \omega^2(\lambda_1 + \lambda_2)^2} \\
&= \frac{1}{(\omega^2 - \det(A))^2 + \omega^2(\mathrm{Tr}(A))^2}
\end{aligned} \tag{A.20}$$

This form for the power spectrum shows clearly the existence of a resonance: for a specific value of ω^2 the denominator becomes small, and the power spectrum has a large peak centered on this frequency. The condition $dP_i(\omega)/d\omega = 0$ gives:

$$2(\omega^2 - \det(A))2\omega + 2\omega(\text{Tr}(A))^2 = 0 \tag{A.21}$$

Then the condition (A.21) simply becomes: $\omega^2 = \det(A) - \frac{(\text{Tr}(A))^2}{2}$, it implies that: $2\det(A) > (\text{Tr}(A))^2$, this condition in terms of the stability matrix implies that the eigenvalues of A are complex. It means that if the power spectrum has an extreme the stability matrix has complex eigenvalues.

Replacing in the expression for the power spectrum the eigenvalues for the model of the system in basal conditions: $\lambda_1 = \frac{-k_2}{2} + i\sqrt{k_2 k_4 - \frac{k_4^2}{4}}$ and $\lambda_2 = \frac{-k_2}{2} - i\sqrt{k_4 k_2 - \frac{k_4^2}{4}}$

$$P_i(\omega) \propto \frac{1}{\omega^4 + \omega^2(k_4^2 - 2k_4 k_2) + k_4^2 k_2^2} \tag{A.22}$$

$$P'_i(\omega) \propto \frac{4\omega^3 + 2\omega(k_4^2 - 2k_4 k_2)}{(\omega^4 + \omega^2(k_4^2 - 2k_4 k_2) + k_4^2 k_2^2)^2} = 0 \tag{A.23}$$

$P_i(\omega)$ has an extreme in $\omega = \sqrt{k_4 k_2 - \frac{k_4^2}{2}}$

As we can see, the imaginary part of the eigenvalues ($\text{Im}[\lambda_{1,2}]$) and the value of frequency where $P_i(\omega)$ has an extreme are similar. Now we are going to write it in a more clearly way:

$$\text{Im}[\lambda_{1,2}] = \sqrt{k_2 k_4 - \frac{k_4^2}{4}} = \sqrt{k_2 k_4}\sqrt{1 - \frac{k_4^2}{4k_2 k_4}}$$
$$\approx \sqrt{k_2 k_4}\left(1 - \frac{k_4^2}{8k_2 k_4}\right) \tag{A.24}$$

The above Taylor expansion may be a good approximation if we take into account that for the corresponding values of the parameters $\frac{k_4^2}{4k_2 k_4} < \frac{k_4^2}{2k_2 k_4} < 0.5$.

In the same way:

$$\omega = \sqrt{k_4 k_2 - \frac{k_4^2}{2}} = \sqrt{k_2 k_4}\sqrt{1 - \frac{k_4^2}{2k_2 k_4}}$$
$$\approx \sqrt{k_2 k_4}\left(1 - \frac{k_4^2}{4k_2 k_4}\right) \tag{A.25}$$

Summarizing, the power spectrum of the fluctuations has a maximum at a frequency close to the imaginary part of the eigenvalue that characterizes the frequency of the damped oscillations in the deterministic regime.

References

[1] Vogelstein B, Lane D and Levine A J 2000 Surfing the p53 network *Nature* **408** 307–10
[2] Junttila M R and Evan G I 2009 p53- a jack of all the trades but master of none *Nat. Rev.* **9** 821–9
[3] Bensaad K, Tsurita A, Selak M A, Calvo M N, Nakano K, Bartrons R, Gottlieb E and Vourden K H 2006 Tigar, a p53-inducible regulator of glycolysis *Cell* **126** 107–20

[4] Sherr C J and Weber J D 2000 The arf/p53 pathway *Curr. Opin. Genetics Dev.* **21** 485–95

[5] Vourden K H and Ryan K M 2009 p53 and metabolism *Nat. Rev.* **9** 691–700

[6] Kibbutat M H G and Vousden K 1998 Keeping an old friend under control: regulation of p53 stability *Mol. Med. Today* **4** 250–6

[7] Lahav G, Rosenfeld N, Sigal A, Geva-Zatorsky N, Levine A, Elowitz M B and Alon U 2004 Dynamics of the p53-mdm2 feedback loop in individual cells *Nat. Genetics* **36** 147–50

[8] Geva-Zatorsky N *et al* 2006 Oscillations and variability in the p53 system *Mol. Syst. Biol.* **2** 0033

[9] Geva-Zatorsky N, Detel E, Batchelor E, Lahav G and Alon U 2010 Fourier analysis and system identification of the p53 feedback loop *Proc. Natl Acad. Sci.* **107** 13550–5

[10] Loewer A, Bachtelor E, Gaglia G and Lahav G 2010 Basal dynamics of p53 reveal transcriptionally atenuated pulses in cycling cells *Cell* **142** 89–100

[11] Batchelor E, Loewer A, Mock C and Lahav G 2011 Stimulus-dependent dynamics of p53 in single cells *Mol. Syst. Biol.* **7** 1–8

[12] Abou-Jaoud W, Ouattara D A and Kaufman M 2009 From structure to dynamics: frequency tuning in the p53-mdm2 network I. Logical approach *J. Theor. Biol.* **258** 561–77

[13] Ouattara D A, Jaoudé W A and Kaufman M 2010 From structure to dynamics: frequency tuning in the p53-mdm2 network II. Differential and stochastic approaches *J. Theor. Biol.* **264** 1177–89

[14] Kim J K and Jackson T L 2013 Mechanism that enhance sustainability of p53 pulses *Plos One* **8** e65242

[15] Jensen M H, Tiana G and Sneppen K 2002 Time delay as a key to apoptosis induction in the p53 network *Eur. Phys. J.* B **29** 135–40

[16] Ma L, Wagner J, Rice J J, Hu W, Levine A J and Stolovitzky G A 2005 A plausible model for the digital response of p53 to dna damage *Proc. Natl Acad. Sci.* **102** 14266–71

[17] Liu B, Yan S and Wang Q 2011 Intrinsic noise and hill dynamics in the p53 system *J. Theor. Biol.* **269** 104–8

[18] Proctor C J and Gray D A 2008 Explaining oscillations and variability in the p53-mdm2 system *BMC Syst. Biol.* **2** 1–20

[19] Cruz L, Figueroa-Morales N, Mulet R and Pinero J 2011 Effects of the intrinsic noise in the dynamics of the mdm2-p53 module *Rev. Cub. Fis.* **2** 23–37

[20] Gillespie D T 1977 Exact stochastic simulation of coupled chemical reactions *J. Phys. Chem.* **81** 2340–61

[21] van Kampen N G 1981 *Stochastic Processes in Physics and Chemistry* (Amsterdam: Elsevier)

[22] Elf J and Ehrenberg M 2003 Fast evaluation of fluctuations in biochemical networks with the linear noise approximation *Genome Res.* **13** 2475–84

[23] Scott M 2011 Applied stochastic processes in science and engineering. Lectures notes

[24] McKane A, Newman T, Nagy J and Stefanini M 2007 Amplified biochemical oscillations in cellular systems *J. Stat. Phys.* **128** 165–91

[25] McKane A J and Newman T J 2005 Predator-prey cycles from resonant amplification of demographic stochasticity *Phys. Rev. Lett.* **94** 218102

[26] Figueroa-Morales N, León K and Mulet R 2012 Stochastic approximation to the specific response of the immune system *J. Theor. Biol.* **295** 37–46

[27] Branzei D and Foiani M 2008 Regulation of dna repair throughout the cell cycle *Nat. Rev. Mol. Cell Biol.* **9** 297–308

[28] Sancar A, Lindsey L A, Unsl-Kacmaz K and Linn S 2004 Molecular mechanism of mammalian dna repair and the dna checkpoints *Annu. Rev. Biochem.* **73** 39–98

[29] Colquhon D 2006 The quantitative analysis of drug-receptor interactions: a short history *Trends Pharmacol. Sci.* **27** 149–57

[30] Weiss J N 1997 The hill equation: uses and misuses *Fed. Am. Soc. Exp. Biol.* **11** 835–41

[31] Batchelor E, Mock C S, Bahn I, Loewer A and Lahav G 2008 Recurrent initiation: a mechanism for triggering p53 pulses in response to dna damage *Mol. Cell* **30** 277–89

[32] Harris S and Levine A J 2005 The p53 pathway: positive and negative feedback loops *Oncogene* **24** 2899–908

[33] Clairambault J, Elia J, Dimitrio L and Natalini R 2014 Dynamics of p53 in single cells: physiologically based ode and reaction-difusion pde models *Phys. Biol.* **11** 045001

[34] Ciliberto A, Nowak B and Tyson J J 2005 Steady state and oscillations in the p53/mdm2 network *Cell Cycle* **4** 488–93

[35] Lain S, van Leeuwen I M M and Chaplain M A J 2009 Spatio temporal modelling of the p53-mdm2 oscillatory system *Math. Model Natl Phenom.* **4** 97–116

[36] Cai X and Yuan Z-M 2009 Stochastic modelling and simulation of the p53-mdm2/mdmx loop *J. Comput. Biol.* **16** 917–33

[37] van Kampen N G 1976 Stochastic differential equations *Phys. Rep.* **24** 171–228